Geochemistry, Classification and Geotectonic Studies of Pan-African Rocks Around Akure, Southwestern Nigeria

[1]Romanus Obasi, [1]Henry Madukwe and [2]Olajumoke Adewumi
[1]*Department of Geology, Ekiti State University, Ado Ekiti, Nigeria*
[2]*Department of Mineral Resources Engineering, The Federal Polytechnic, Ado-Ekiti, Nigeria*

Key words: Classification, fractionation, geochemistry, geotectonics, mixed sources

Corresponding Author:
Romanus Obasi
Department of Geology, Ekiti State University, Ado Ekiti, Nigeria

Abstract: The study of geochemistry, classification and geotectonics of granitic rocks of Akure, Southwestern Nigeria are undertaken. Geochemical analysis classified the rocks suites as quartz-rich, silica-saturated, alumina-saturated, dorminant peraluminous, S-type, slightly metaluminuos, I-type and A-type granites. A plot of total alkalies-silica of alkaline and sub-alkaline rock suites indicated granite, syenite, quartz-diorite, gabbro, monzogranite and monzodiorite as rock types. The sub-alkaline rocks exhibited evidence of crystal fractionation from a magmatic melt generated by partial melting of basaltic materials. The Y/Nb ratio (1.39-7.03 1.2) affirmed that magmas that produced the rocks were either derived from crustal or mixed sources. Significant variations in the correlation of Sr, Zr, Ba and Rb with SiO_2 suggested the involvement of more than one sources in the genesis of the rocks. The depletion of Ba (0.48-8.76), the presence of distinct negative Eu in the REE pattern, with a strong negative correlation of Al_2O_3 and CaO with increasing SiO_2 are characteristics suggestive of an extensive fractionation of plagioclase. These rocks were involved in the active magmatic and tectonic activities with post collision uplift and late orogeny that were in conformity with the tectonic scenario of Pan-African granite. These geodynamic activities resulted in the emplacement of granitic rocks suites into the host rock.

INTRODUCTION

The areas of study, Akure and its environs form parts of the Southwestern Nigerian Basement Complex. The complex consists of several lithogeological units namely migmatite-gneiss quartzites complex, the schist belts (metasediments), the Pan African granites (Older granites) and late intrusives. These rock units were subjected to polycyclic deformations and intruded by syn-and post-orogenic granitoids. The Pan African rocks are wide spread around Akure and environs and its geology also widely studied. During the Pan African orogeny[1], they intruded into the pre-existing migmatites gneiss quartzite complex and metasediments (schist) of Liberian (2700

Ma), Eburnean (2000-2700 Ma) and probably Kibaran (1100 Ma) ages. During this orogenies, many rock suites of granitic family were emplaced into the existing host rocks. Rock samples were taken from among these rock suites and geochemically analyzed. The analysis gave knowledge of the tectonic events that produced the granitic rocks, the magma and its sources. The present study is aimed at determining the geochemistry, petrogenesis and the geotectonics of the rocks. The data would determine the magmatic sources, fractionation trends, rock classifications and geotectonic episodes as well as environment of rock emplacement.

MATERIALS AND METHODS

Field relationships: The 20 rock samples were collected from several rock exposures around Akure and its environs. The textures and colours were examined. Figure 1 shows some of the photographs taken from the field. Figure 1a (shows pink, white and dark colours of a fine-grained granite), Fig. 1b: (white, grey and dark; fine-medium grained, quartz vein intruded into the host granitoid); Fig. 1c (porphyritic granite, medium to coarse grained); Fig. 1d (pinkish quartz veinlets intruded into dark rock); Fig. 1e (medium grained rock); Fig. 1f (fine
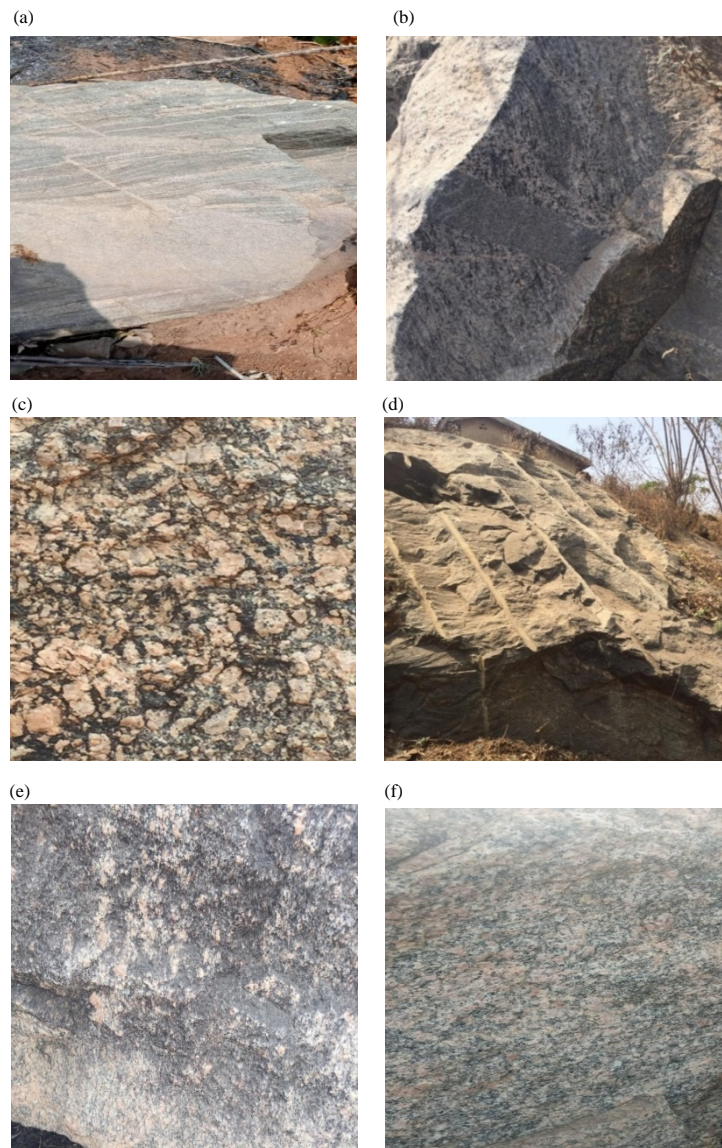

Fig. 1(a-f): Shows some of the cuttings from the field, (a) Shows pink, white and dark colours, fine-grained granite, (b) White, grey and dark; fine-medium grained, quartz vein intruded into the host granitoid, (c) Porphyritic granite, medium-coarse grained, (d) Pinkish quartz tiny-intruded veins resting on dark rock, (e) Medium grained rock) and (f) Fine grained rock

Table 1: Whole rock composition of the Akure granitic rock

Samples	1	2	3	4	5	6	7	8	9	10	Mean
SiO_2	71.65	73.12	59.84	71.40	64.73	98.92	57.85	74.32	50.18	64.43	68.64
A_2O_3	14.64	13.64	15.09	13.47	15.26	0.26	15.57	12.27	15.65	17.29	13.31
Fe_2O_3	2.83	3.50	8.03	3.91	6.51	0.52	9.00	3.82	10.77	4.76	5.37
K_2O	5.98	4.57	4.22	5.69	5.49	0.07	3.53	5.17	1.16	3.66	3.95
Na_2O	3.28	3.49	3.22	3.00	3.22	0.02	3.29	2.57	2.63	4.27	2.90
MgO	0.09	0.21	1.55	0.31	0.71	0.00	2.39	0.01	7.99	1.10	1.44
CaO	1.35	1.32	4.85	1.57	2.97	0.04	5.48	1.25	9.87	3.87	3.26
MnO	0.03	0.04	0.10	0.05	0.10	0.02	0.11	0.05	0.15	0.08	0.07
TiO_2	0.20	0.29	1.62	0.45	0.86	0.11	1.80	0.35	1.59	0.53	0.23
P_2O_5	0.05	0.10	0.61	0.13	0.25	0.01	0.69	0.03	0.32	0.13	0.23
LOI	-0.25	0.09	0.33	0.26	-0.24	-0.10	0.13	-0.04	0.24	0.00	0.04
Sum of conc.	99.86	100.38	99.46	100.24	99.86	99.87	99.84	99.80	100.64	100.12	100.01

grained rock). Some rocks are in ridges, some massive and others are in form of inselbergs. The GPS readings were taken at each location of sampling.

Preparation and analytical technique: The samples were pulverized at the Geology Engineering laboratory of Ekiti State University, Ado Ekiti. The powdered samples were then taken to the University of Stellenbosch Central laboratory for the major, trace and rare earth analyses. The major oxides were analyzed using the XRF Rh Tube 3k Watt, (PANalytical AXIOUS PW4400/40 spectrometer) at the Central Laboratory of the University of Stellenbosch, South Africa while the trace and the rare earth elements were analyzed using the Laser ablation ICP-MS (Perkin-Elmer Sciex ELAN DRC 6000) at the Central Laboratory of the University of Stellenbosch, South Africa.

Routine methods for sample digestion and preparation of solutions for ICP-MS were that of Balaram *et al*.[2]. The international rock standards (USGS) used for calibrations for both WD-XRF and La ICP-MS are JG-2 and DG-H.LOI (loss on ignition) is the total of volatiles content of the rock including the water combined to the lattice of silicate minerals) and the gain on ignition related to the oxidation of the rock (mostly due to Fe). Details of ICP-MS and laser operating methods and conditions have been published by Norman *et al*.[3, 4]. The results of the XRF geochemical analysis are presented in Table 1.

RESULTS AND DISCUSSION

The results of the analysis of the Pan African rocks show varying concentrations as indicated in Table 1 The analysis shows that silica, SiO_2 ranges from 50.18-71.65, alumina, A_2O_3 (0.26-17.29), Fe_2O_3 (0.52-10.77) and potash, K_2O (0.07-5.98). The high value of the alumina, (Al_2O_3) 0.26-17.29 resembles those of the calc-alkaline rock series[5] but the mean value of Al_2O_3(13.31) is lower than the average crustal value (15.6) an indication of its depletion in the crust (Table 2). The mean value of K_2O (1.69) is lower than the crustal mean value of 2.5 showing its depletion also in the crust.

The mean values of Na_2O, MgO and CaO are 2.90, 1.44 and 3.26, respectively and are lower than the crustal values of 3.2, 3.9 and 5.8, respectively equally indicating impoverishment in the crust. However, P_2O_5 has a higher value of 0.23 than that of the crust (0.11) showing its level of abundance in the crust. K_2O is comparably in excess of Na_2O with the ranges of 0.07-5.98 and 0.02-4.27, respectively. TiO_2 is generally below 1% except in samples 3, 7 and 9 where the concentrations are slightly >1. Those samples that are <1% are within the range acceptable in calc-alkaline lavas of Irvine and Barager[6] and Pearce and Cann[7]. Jakes and White[8] suggested that when CaO values are higher than 3% in the rock, there is the likelihood of the presence of epidote and non-metamorphism of such rocks in those areas. In the rocks under study six samples: 1, 2, 4, 5, 6 and 8 have CaO values of <3% while the other 4 samples have values that are >3% which means that majority of the rocks suites underwent metamorphism.

It is observed that the immobile oxides of Al_2O, Fe_2O and TiO_2 have higher concentration than the mobile oxides of K^+, Na^+ Mg^+. The ratio of Fe_2O_3/MgO varies from 0.00-382% reflecting an abundant secondary opaque phase magnetite in relation to magnesia. The ratio of Na_2O/K_2O ranges between 0.29 and 2.27% and relatively low when compared with the values proposed by Jakes and White[9] for calc-alkaline rocks. However, the low values reflect a depletion during alteration and metamorphism of those rocks.

Classifications of rocks from Akure: There are a number of rock classifications involving the use of different methods, one of which is the felsic-mafic ratio (F) and the silica saturation ratio (S) method, together written as F-S method. F is defined in Eq. 1 as:

$$F = \frac{SiO_2 + Na_2O + K_2O \text{ in wt.\%}}{Fe_2O_3 + MgO + CaO}$$

Segerstrom and Young while S is defined in Eq. 2 as:

Table 2: Major element composition and some ratios

Samples	1	2	3	4	5	6	7	8	9	10	CA
SiO_2	71.65	73.12	59.84	71.40	64.73	98.92	57.85	74.32	50.18	64.43	60.3
A_2O_3	14.64	13.64	15.09	13.47	15.26	0.26	15.57	12.27	15.65	17.29	15.6
Fe_2O_3	2.83	3.50	8.03	3.91	6.51	0.52	9.00	3.82	10.77	4.76	7.2
K_2O	5.98	4.57	4.22	5.69	5.49	0.07	3.53	5.17	1.16	3.66	2.5
Na_2O	3.28	3.49	3.22	3.00	3.22	0.02	3.29	2.57	2.63	4.27	3.2
MgO	0.09	0.21	1.55	0.31	0.71	0.00	2.39	0.01	7.99	1.10	3.9
CaO	1.35	1.32	4.85	1.57	2.97	0.04	5.48	1.25	9.87	3.87	5.8
MnO	0.03	0.04	0.10	0.05	0.10	0.02	0.11	0.05	0.15	0.08	0.10
TiO_2	0.20	0.29	1.62	0.45	0.86	0.11	1.80	0.35	1.59	0.53	1.0
P_2O_5	0.05	0.10	0.61	0.13	0.25	0.01	0.69	0.03	0.32	0.13	0.11
LOI	-0.25	0.09	0.33	0.26	-0.24	-0.10	0.13	-0.04	0.24	0.00	-
Sum of conc.	99.86	100.38	99.46	100.24	99.86	99.87	99.84	99.80	100.64	100.12	-
Na_2O/K_2O	0.55	0.76	0.76	0.53	0.59	0.29	0.93	0.50	2.27	1.17	-
Al_2O_3/Na_2O+ $CaO+K_2O$	1.38	1.45	1.23	1.31	1.31	2.00	1.27	1.36	1.15	1.47	-
Na_2O+K_2O	9.26	8.06	7.44	8.69	8.71	0.09	6.82	7.74	3.79	7.93	-
SiO_2/Na_2O	21.84	20.95	18.58	23.8	20.10	4946.	17.58	28.92	19.08	15.09	
Fe_2O_3/Fe_2O_3+ MgO	0.97	0.94	0.84	0.93	0.90	1.00	0.79	0.99	0.57	0.81	-
A_2O_3/Na_2O+K_2O	1.58	1.69	2.03	1.55	1.75	2.29	2.28	1.59	4.13	2.19	-
K_2O/Na_2O	1.82	1.31	1.31	1.89	1.70	3.5	1.07	2.01	0.44	0.86	-
Fe_2O_3/MgO	31.44	16.67	5.18	12.61	9.17	0.00	3.77	382.0	1.35	4.33	-
$Na_2O+CaO+$ K_2O/Al_2O	0.72	0.69	0.81	0.76	0.77	0.50	0.79	0.73	0.87	0.68	-

Table 3: Values of the present work and the standard values of F and S

Rock	Present work		Values of F and S	
	F	S	F	S
Ultrafelsic granite (Ultrafelsic rhyolite)	18.95	2.54	33.7	2.92-3.05
Felsic granite (Felsic rhyolite)	16.14	2.74	23.6-33.7	2.69-2.92
Granite (rhyolite)	4.66	1.93	15.2-23.6	2.35-2.46
Adamellite (quartz latite)	13.83	2.55	9.62-15.2	2.12-2.06
Granodiorite	7.21	1.89	6.80-9.62	2.05-1.82
Tonalite (dacite)	176.80	108.70	4.52-6.80	1.31-1.24
Monzonite	3.83	1.47	2.98-4.52	1.15-1.26
Diorite (andesite)	16.15	2.96	2.14-2.98	0.98-1.11
Gabbro (basalt)	1.89	1.04	1.51-2.14	
Ultramafic	7.44	1.84	<1.51	

Values of F and S Nockolds[10]

$$S = \frac{SiO_2}{Al_2O+Na_2O+CaO+K_2O+MgO+Fe_2O_3} \qquad (2)$$

The F-S method has been used to yield compositional equivalent names that correlate with average rock types of Nockolds[10] and the petrogenetic inference of the rocks. The F-S methods of Nockolds[10] tend to bring out the compositional equivalent of rock types using the worked out values of F and S (values in the present work that match F-S values). Using Table 3, the values of 176.80 and 108.70 under F and S of the present work are >33.7 and 2.92-3.05 (Table 3) indicating that particular sample is from the rock type ultrafelsic granite. The values 18.95,16.14 and 16.15 of the present work fall within the range of 15.2-23.6 under the F of the standards signifying that the compositional equivalent of the rock type is granite (Rhyolite). Data F (7.21 and 7.44) from the present work show a compositional equivalent of granodiorite and under S = 1.89. Other compositional equivalent rock types are; F = 4.66 falling into tonalite

(dacite) S = 2.05-1.82. These compositional equivalents indicate collectively that the rocks are of granitic family (granitoid).

A plot of F-S in Fig. 2 indicated some rock suites. A plot of total alkalies-silica diagram (Fig. 3) of Le Bas *et al*.[11] showed fields and examples of alkaline and sub-alkaline rock suites in support of the compositional rock equivalents. The vertical dashed lines separate the alkaline from the sub-alkaline while the thick dashed curved lines separate the rock types. The samples plotted on the granite, slightly on the syenite and quartz-diorite as well as gabbro, all within the sub-alkaline rock suite.

It is observed here that the rock suites range from basic (gabbro) intermediate (syenite) to acidic (granite), respectively.

However, another plot of R1 versus R2 (Fig. 4) showed that the samples fell into the monzogranite, monzodiorite, tonalite and gabbro fields. The different rock type names observed from these plots point to the fact that a rock may be given one name on the ground of
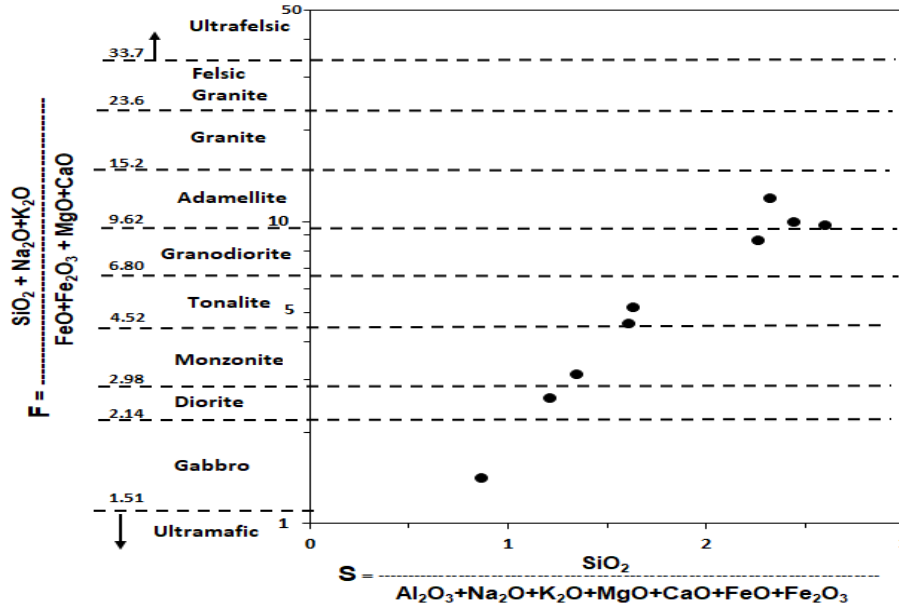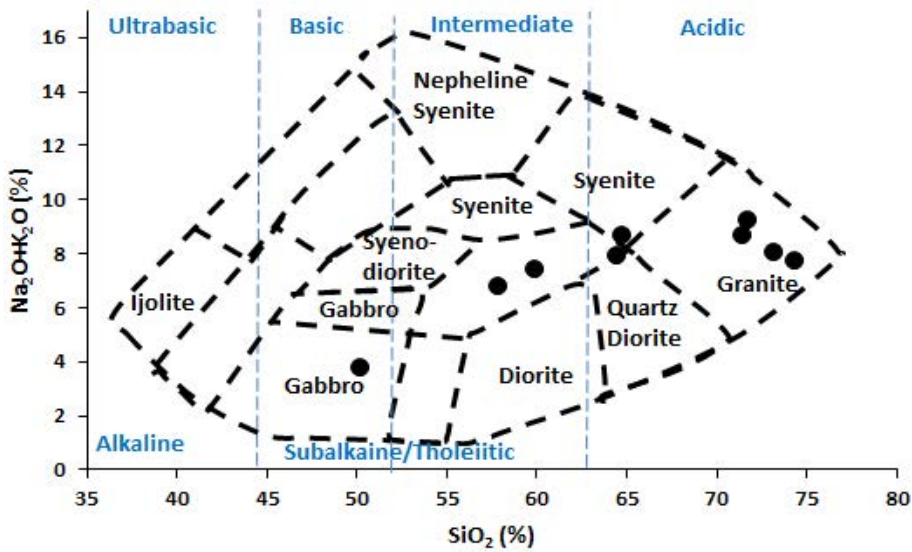
Fig. 2: A plot of F versus S

Fig. 3: A plot of the total alkalies-silica diagram showing fields and examples of subalkaline Alkaline rock suites[11]

field occurrence and from hand lens examination and another when studied in thin section and perhaps another name when chemically analyzed[12]. The fact remains that all the rock types belong to the granite family and widely sub-alkalinesuites. The fields so plotted may not be so discrete because no natural division exists inrocks and so, classification therefore serves as a means of systematizing information just as Williams *et al*.[12] reported that different schemes have

different objects in view. The degree of silica saturation in a crystallizing magma of the rocks under study can be ascertained by using the molar ratio of SiO_2/Na_2O. The molar ratio of SiO_2/Na_2O ranges from 15.09-4946. 0. Under the concept of the degree of silica saturation, if there is an excess of molar SiO_2 in relation to the one needed to make albite from Na_2O under ratio $SiO_2/Na_2O>6$, then the magma can crystallize quartz along with albite. The rocks under study have SiO_2/Na_2O
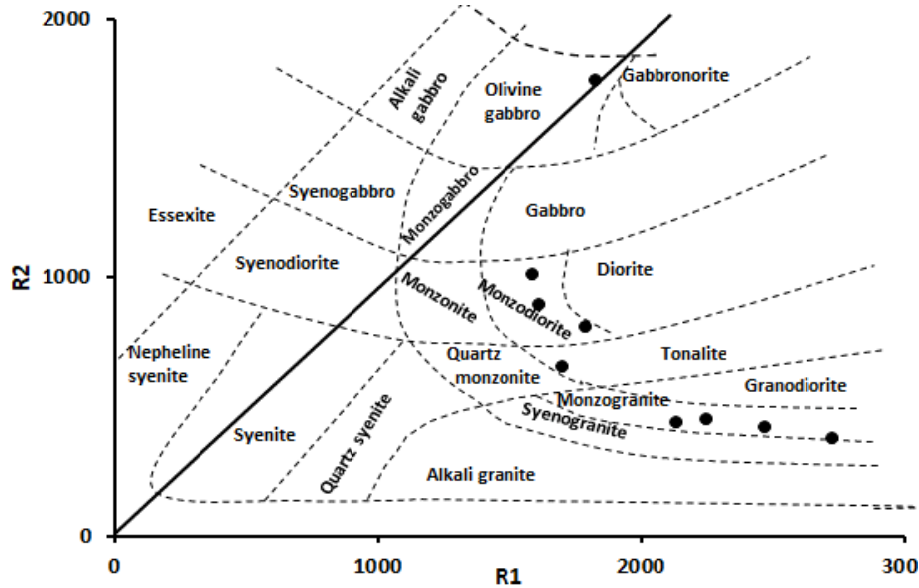
Fig. 4: A plot of R2 versus R1

ratio that are >6, therefore, the magma and the corresponding rocks are silica over-saturated. Silica-oversaturated rocks contain normative minerals Q, (quartz or its polymorphs) cristobalite and tridymine of granite family. The silica concentration in the rock analyzed indicates that the rocks fall into the acid class of 66[13]. Acid rocks are silicic. The rocks under study are also quartz-rich and over-saturated (Fig. 5).

When the ratio of $K_2O/Na_2O>1$ and $K_2O>Na_2O$ it means that the source of the rock is either from an igneous or metamorphic source and this applies to the present study.

The Fe-number or Fe^* is another means of classifying the granitic granites by using the plot of Fe_2O_3/F_2O_3+MgO versus SiO_2. (Miyashiro, 1970). The Fe-number is the ratio of Fe_2O_3/F_2O_3+MgO versus SiO_2 in relation to the variations of silica content. Samples on the plot of Fe_2O_3/F_2O_3+MgO versus SiO_2 clustered on the ferran field (Fe-rich) while a sample lied on the Magnesian field (Fig. 6). Tholeiitic rocks show very strongenrichment in Fe relative to Mg than in calc-alkaline rocks (Fig. 7). The calc-alkaline suite on its own shows enrichment in silica and alkalies[14]. Tholeiitic and calc-alkaline rocks indicate subduction zones whereas the calc-alkaline suite with less Fe enriched basalt andesite and rhyolite develop on very thick continental crust above subduction zone[14].

Shahabpour[15] related the magnesian type of granitoids to cordillerian granitic rocks while the ferran and magnesian coupled with the leucocratic, potassic and ultrapotassic rocks belong to four families of the
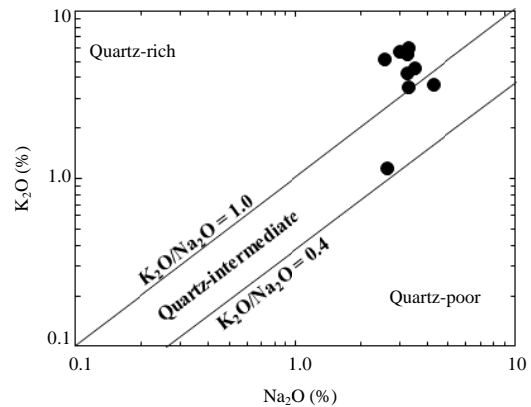

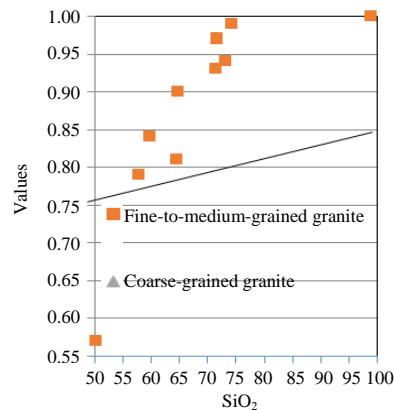Fig. 5: K_2O versus Na_2O plot

Fig. 6: Fe_2O_3/F_2O_3+MgO versus SiO_2 plot[15]

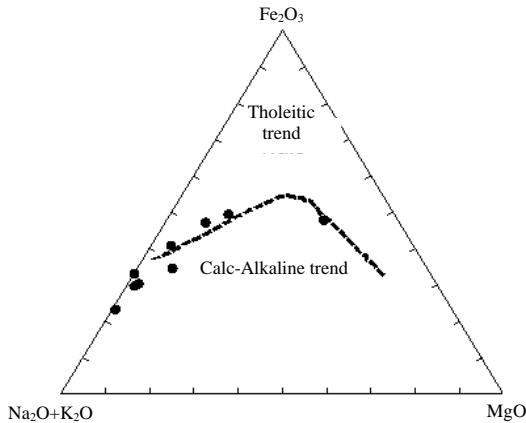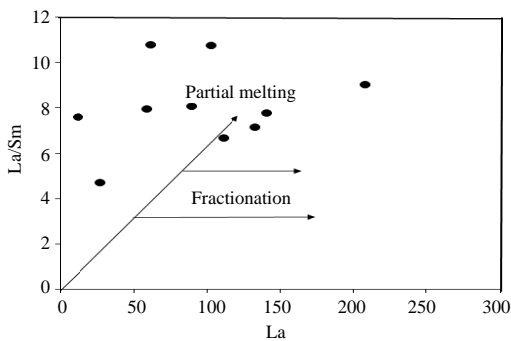Fig. 7: A FeO*-Alk-MgO triangular diagram for dissociation of tholeiitic and calc-alkaline series[6]

Fig. 8: A plot of La/Sm versus La showing partial melting and fractionation[16, 17]

feldspathic rocks[18]. In order to identify the enrichment of Ferroan and magnesian in a rock, use is made of Fe-number<0.5. Magnesian is abundant if Fe-number<0.5 and if this number is exceeded it means an abundant Fe. The ratio of Fe_2O_3/F_2O_3+MgO in the study areas ranges between 0.57 and 1.00, implying that the Akure rocks are ferron granitic rocks (Fe-rich). Ferron granitic rocks are associated with low oxygen fugacity during melting[17]. Interestingly, most Fe-rich granitic rocks form by differentiation or partial melting of the basaltic parents[16, 17] (Fig. 8). The plot of K_2O against SiO_2 shows that the rock samples plotted on the high-K calc-alkaline and the shoshonite fields and scantly on the low-K tholeiite and medium K-calc-alkaline (Fig. 9). Robert and Clemens[19] and Ukaegbu[20] reported that granites of all types are products of partial melting of hydrous calc-alkaline to high-K calc mafic within the crust. This is corroborated by Fig. 8 in which most of the samples plotted in the partial melting field.
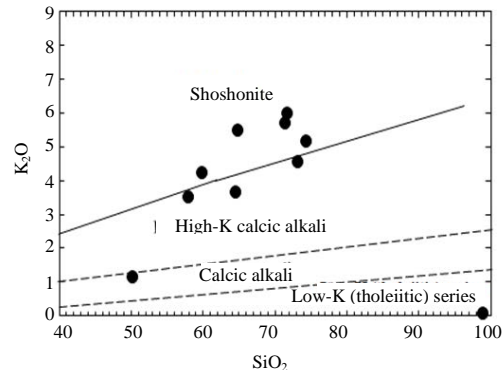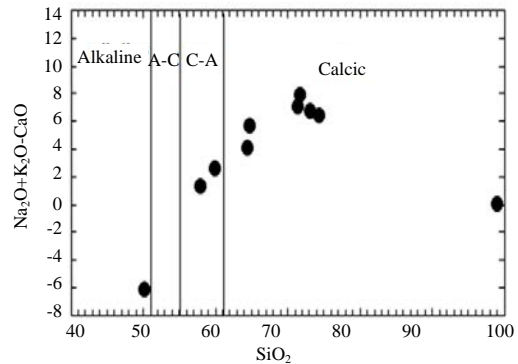

Fig. 9: Plot of K_2O against SiO_2[21]

Fig. 10: Na_2O+K_2O-CaO versus SiO_2 plot[22]

The rocks can be classified as calcic based on the cross-plots of Na_2O+K_2O-CaO versus SiO_2. Peacock[22], though, some of the samples plotted slightly on the Calc-Alkaline (CA) and alkaline fields (Fig. 10). Similarly, samples plotted on the calcic and calc-alkaline as shown in Fig. 11 in cross- plot of (Na_2O+K_2O-CaO) vs. SiO_2 diagrams[23].

Using the plots of Na_2O+K_2O-CaO vs. SiO_2[23], the rock samples clustered into the fields of calcic and calcic-alkali in line with the Modified Alkali-Lime Index (MALI) classification. The MALI classification is used to classify volcanic suites of rocks into calcic, calcic-alkali, alkali-calcic and alkali (Fig. 11). It is noted that when SiO_2 content at which the alkalies, Na_2O+K_2O in a suite of lava is equal to CaO, the rock suites whose alkali-lime index is >61 is referred to as calcic, if the index is between 56 and 61, it is calc-alkalic, from 51-56, the suites are alkali-calcic and <51, they are alkali.

Alumina, A_2O_3 is the second abundant constituent after silica in most magmatic rocks and it is another means of classification especially for felsic rocks such as granitic types. Maniar and Piccoli[24] have used the Alumina Saturation Index (ASI) defined as the molar ratio
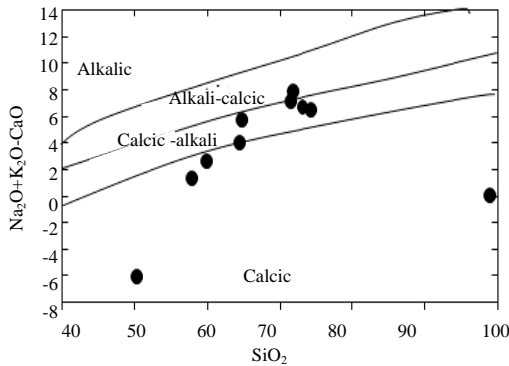
Fig. 11: MALI-index (Na₂O+K₂O-CaO) vs. SiO₂ diagrams[23]

$Al_2O_3/Na_2O+CaO+K_2O$ (A/CNK) to classify the felsic rocks. When magmas crystallizing feldspar and/or feldspathoid have ASI>1.1, Al_2O_3 must be accommodated in mafic or in the aluminous accessory minerals such as cordierite, sillimanite andalusite, corundum as well as Al-rich biotite. Rocks which have excess of this Al_2O_3 are said to be alumina-saturated or peraluminous. The rocks under study have mol. $Al_2O_3/Na_2O+CaO+K_2O>1.1$ with the ASI ranging from 1.14-2.00 and an average of 1.39 making the rock to be classified as peraluminous (Table 2). However, a plot of Al/CNK against Al/NK diagram in Fig. 12 showed that the samples are slightly metaluminuos, I-Type and mostly peraluminous (1.14-2.00) S-Type. A plot of A/CNK against SiO_2 put the samples as S-Type granitoid (Fig. 13). However, samples plotted on the I-type and A-type granites on the plots of K_2O versus Na_2O and $(Na_2O+K_2O)/CaO$wt.% against Zr+Nb+Ce+Y ppm, respectively (Fig. 14 and 15). From all intents and purposes, the rocks under study can be classified as peraluminous, S-type, slightly metaluminuos, I-type and I-type and A-type granites as plotted on K_2O versus Na_2O and $(Na_2O+K_2O)/CaO$wt.% against Zr+ Nb+Ce+Y ppm, respectively. The plotting of samples on ferroan field making the rock ferroan granite and partly magnesian. $(Fe_2O_3/(Fe_2O_3t+MgO))$] vs. SiO_2 diagram (Fig. 6) and on calc-alkalic, calcic fields in the MALI (Na_2O+K_2O-CaO) vs. SiO_2 diagram (Fig. 11) gave the features that agreed with chemical characteristics of worldwide A-type granites. However, the same granitic rocks have high Fe (Fe-rich) and are K-rich having an average of K_2O/Na_2O~1.59 ratios. This implies that the granites in the study area are roughly similar to the peraluminous A-type granites. However, the different fields, so, plotted is an indication of different petrogenetic sources. Corroborating with the views of Loiselle and Wones[16] who originally suggested that A-type granites are formed by fractionation of mantle-derived alkali basalt with or without crustal interaction but Eby[25] reported that A-type granitic melts can form from the mixing of crustal

and mantle sources. Frost and Frost[26] came up with three main modes in the formation of ferroan granitic compositions to include; partial melting of quartz-feldspathic crustal rocks; differentiation of tholeiitic or alkali basaltic magma and a combination of the first two models. With these information, it becomes clearer that the Pan African rocks under study are ferroan, calc-alkalic, metaluminous to peraluminous reduced A-type granites, though some samples show oxidised nature too. Dall'Agnol and de Oliveira[27] were of the opinion that the rocks with the above features enumerated by Eby[25] were either derived from the low-pressure partial melting of quartz-feldspathic igneous sources with a metasedimentary rock input or alternatively from differentiation of tholeiitic sources with significant crustal contamination as proposed by Frost and Frost[26].

The samples plotted on the S-type granitoids field. The different classifications shown by these diagrams indicate the different petrogenetic history of the rock suites.

Figure 16 presents the affinity (Fig. 16). Sub-alkaline rocks are usually silica-saturated or over-saturated and lack normative nepheline.

The SiO_2/Na_2O ratio which is 6 affirms the silica oversaturation of the present study. Sub-alkaline rocks are subdivided into the tholeiitic and calc-alkaline rock suites (Fig. 7). Figure 17 displays the samples that lie on the continental field thus affirming the development of the calc-alkaline on the continental crust. The sub-alkaline rocks show evidence of crystal fractionation from a magmatic melt.

The plots of Na_2O/Al_2O versus K_2O/Al_2O indicate that samples plotted mainly on the igneous field an indication of the magmatic crystallization of the rock (Fig. 18). However, one single sample plotted on the sedimentary and metasedimentary field showing that some of the rocks may have formed through recrystallization of the solid magma. Nonetheless, when the ratio of $K_2O/Na_2O>1$ and $K_2O>Na_2O$ it means that the source of the rock is either from igneous or metamorphic and snot sourced from the sedimentary environments.

The Harker variation diagrams of some major elements of the rocks showing correlation with SiO_2 are presented in Fig. 19a-i. Of particular interest is the strong positive correlation of K_2O with SiO_2 (Fig. 19d) and the negative linear trend of P_2O_5, CaO, MgO, MnO, TiO_2 and Fe_2O_3 with SiO_2 (Fig. 19,b, h, g, f, e and c). Al_2O_3 and NaO_2 have no concrete correlation trend with SiO_2. Figure 19a and i). The decreasing trend of CaO, MgO, TiO_2 and Fe_2O_3 with increasing SiO_2 is a characteristic of a fractionating granitic system.

The variation diagrams using the trace elements show that Sr and Zr correlate negatively with SiO_2 (Fig. 20b and c) while Ba, Rb&REE showed no obvious variation
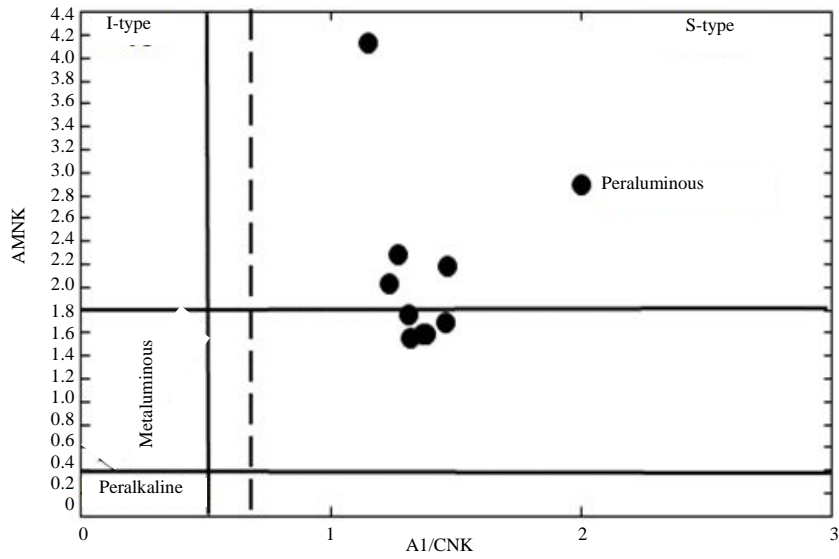
Fig. 12: A Plot of Al/CNK against Al/NK diagram for determination of the aluminum saturation index[24] and dissociation of I and S-type granites[28]
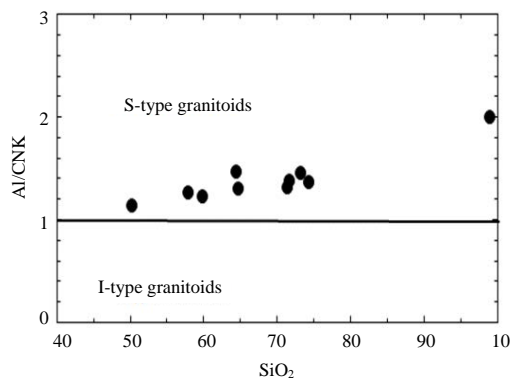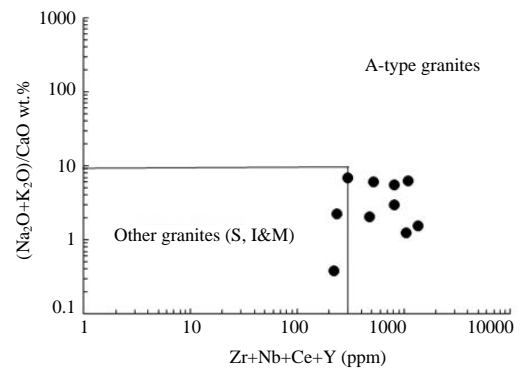

Fig. 13: Plots of Al/CNK versus SiO$_2$

Fig. 15: Granitoid discrimination diagrams from Whalen *et al*.[29] for Akure samples
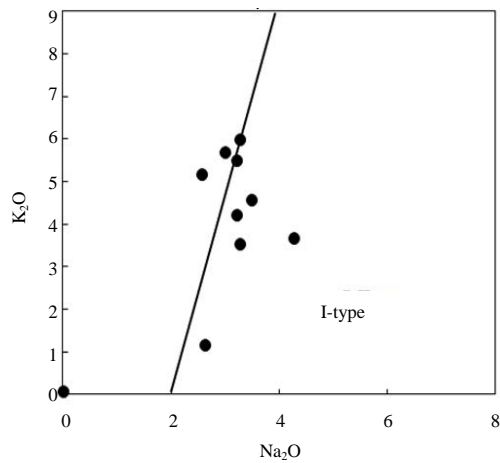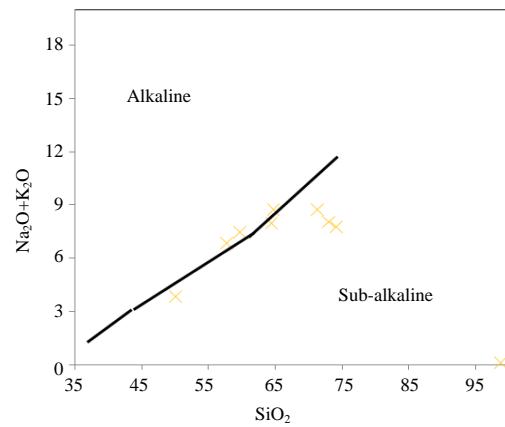

Fig. 14: The plots of K$_2$O versus Na$_2$O

Fig. 16: Alkali-SiO$_2$ discrimination diagram for the Akure granitoids

Table 4: Trace Elements composition in the rocks

| Samples	Ak1	Ak2	Ak3	Ak4	Ak5	Ak6	Ak7	Ak8	Ak9	Ak10
Sr	3.86	11.52	6.16	13.49	16.37	21.06	13.84	14.11	8.61	14.66
V	18.94	46.67	23.5	36.16	45.76	96.74	39.78	45.83	23.96	37.79
Cr	46.67	46.9	84.8	63.75	69.3	78.05	66.95	85.55	98.45	66.25
Co	3.17	7.98	4.03	5.87	6.56	14.87	6.55	7.17	3.27	5.80
Ni	15.7	15.02	7.95	7.40	7.43	15.33	8.86	8.06	7.55	5.76
Cu	88.95	60.14	23.65	18.91	19.08	43.16	27.08	26.49	62.9	20.5
Zn	22.95	60.35	38.35	52.25	67.9	79.55	54.1	55.85	25.5	49.4
Rb	220.6	84.95	110.85	106.15	81.2	97.6	93.75	90.9	106.2	105.65
Sr	165.5	575.1	283.35	425.85	364.75	330.35	433.0	315.8	377.65	406.25
Y	10.73	28.04	26.93	57.44	37.94	62.31	52.7	53.57	24.19	63.43
Zr	163.6	330.2	856.5	997.3	721.95	897.05	925.2	947.95	672.35	1016.75
Nb	7.7	11.52	5.56	10.26	5.82	15.56	7.50	17.06	6.78	14.13
Ba	8.76	3.19	0.85	0.67	0.48	2.09	0.88	2.83	0.75	0.67
Th	31.3	13.24	76.65	77.60	43.62	45.65	73.70	118.45	54.55	84.28
U	2.45	0.80	4.06	4.23	2.58	9.13	4.98	6.06	5.67	12.81
Pb	35.1	33.27	31.85	27.27	31.74	23.62	28.18	29.87	28.2	27.22
Hf	4.64	8.55	23.90	26.56	19.52	23.79	24.58	25.58	19.37	26.93
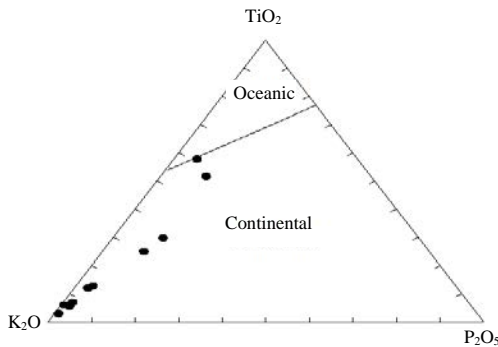
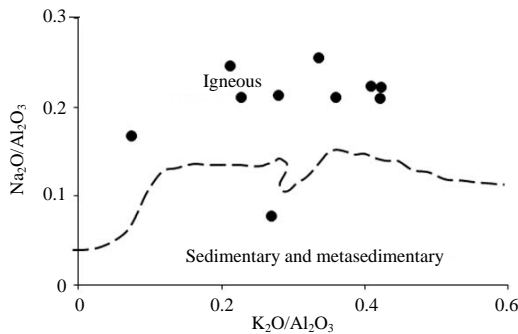Fig. 17: Ternary diagram of the oceanic and continental fields

Fig. 18: Na_2O/Al_2O_3 versus K_2O/Al_2O_3 plots

trends, in which case Sr and Zr decrease with an increasing SiO_2 (Fig. 20b and c). Ba however shows very little correlation with increasing SiO_2 (Fig. 20a. The plot of REE versus SiO_2 also showed no definite correlation trend (Fig. 20e).

These variations significantly suggest the involvement of more than one source in the genesis of the rocks.

Trace and rare earth elements geochemistry: The trace element data are presented in Table 4 showing that the rock has an enriched Rb (81.2-220.6), Zr (163.6-11016.75), Cr (46.67-98.45) and Sr (165.5-575.1) and impoverished Ba (0.48-8.76), Ni (5.76-15.7), Cu (18.91-88.95), Y(10.73-62.31) and Zn (22.95-79-55), respectively. Nb and Y are present in the rock pointing to the importance of arc or subduction related magmatism in the evolution history of the rocks[30, 31]. Eby[25, 32] reported that the ratio of Y/Nb can be regarded as a key to identifying the sources of magma. He stated that Y/Nb ratio 1.2 implies solely crustal sources or mixed sources of the magma. The ratio of Y/Nb (1.39-7.03) in the studied rocks is >1.2 implying therefore that the magmas that produced the rocks were either derived from crustal or mixed sources (Table 4). Y values in the rocks from Akure range from 10.73-63.43 with an average of 41.73 while Taylor (1965) reported 40 ppm for the crust. High concentration of Th (31.3-84.28), U (0.744-12.76) and Pb (23.67-33.27) are features of the involvement of crustal components in the genetic history of the rocks. Again some large ionic lithophile elements (LILE) such as Rb (84.95-220.6), Th (13.24-118.45) and Ce (106.42-390.90) have high concentrations while some high field strength elements (HFSE) like the Nb (5.56-17-06) Zr (163.6-1016.75) and Pr 11-57-43-99) have depleted concentrations. Rocks which have peraluminous characteristics, enriched in LILE coupled with distinct negative European (Eu) anomaly are said to have the characteristics of the Upper crustal domain. The Akure rocks being studied have the presence of these traits and therefore suggests the derivation of the melts from the crustal domain[33, 34]. An enriched Light rare earth elements (LREE) and LILE and depleted HREE and HFSE are also characteristics of typical Arc magmatism of the rocks[35, 36].
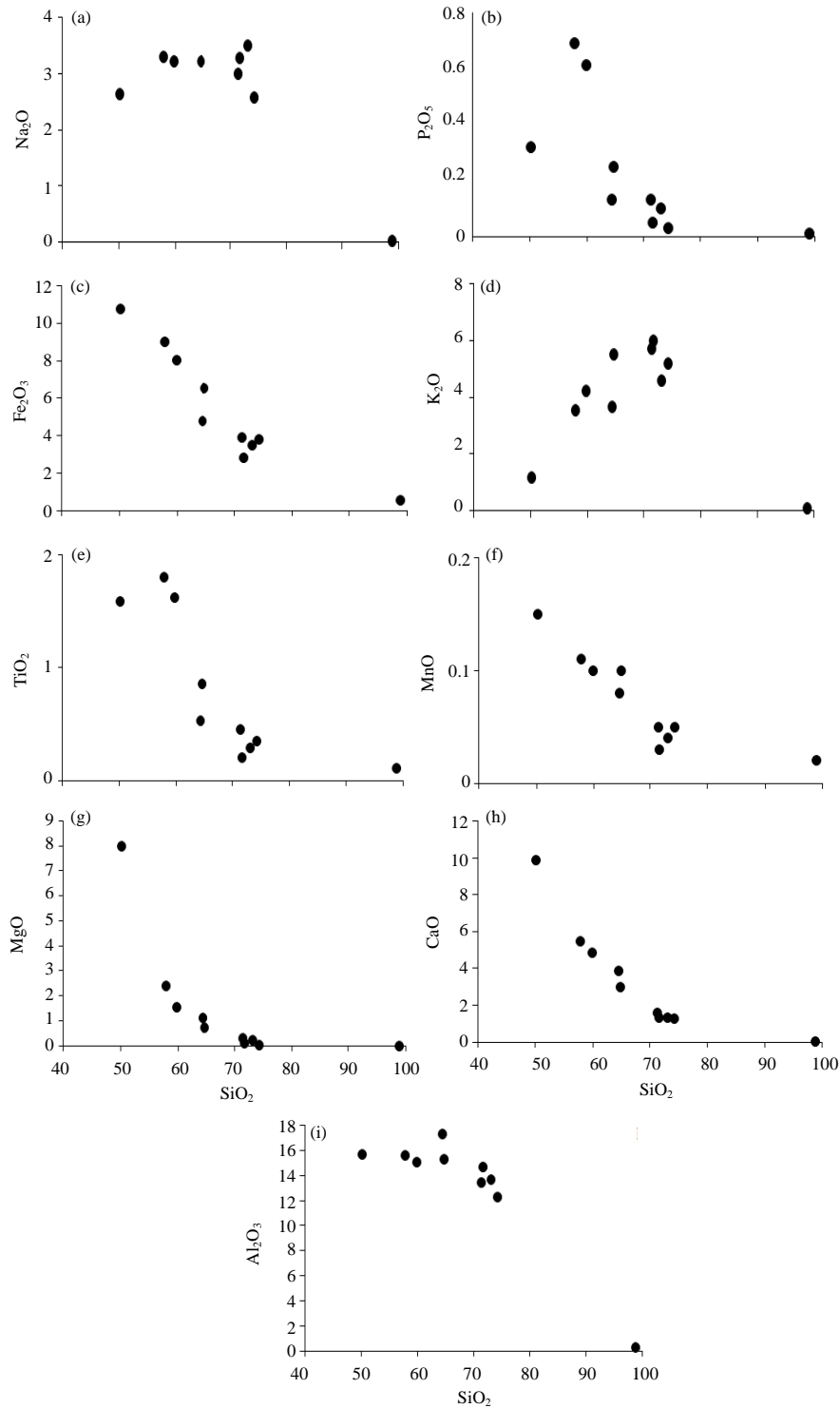
Fig. 19(a-i): Harker variation diagrams of the major element oxides with SiO_2 for granitic rocks of the studied

The REEs abundance of the studied rocks are reported in Table 5 and were normalized to Chondrite following Taylor and Mclennen[37] as presented in Table 6. The REE pattern in Fig. 21 showed a very distinct pattern of a negative slope from LREE to Heavy Rare Earth (HREE) with relatively flat pattern. $((La/Yb)N$
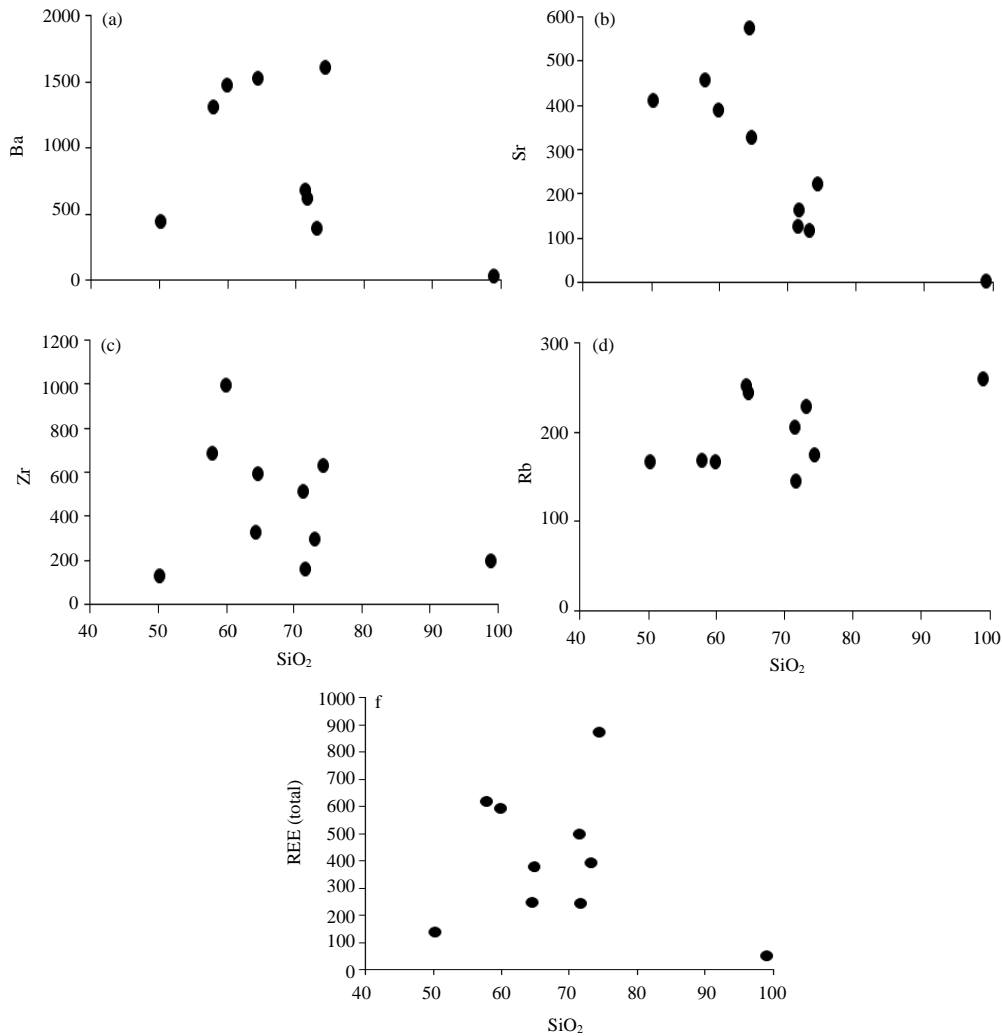
Fig. 20(a-e): Binary diagrams of (a) SiO₂ vs. Ba (b) SiO₂ vs Sr, (c) SiO₂ vs. Zr, (d) SiO₂ vs. Rb& (e) SiO₂ vs. REE showings simple fractionation trends
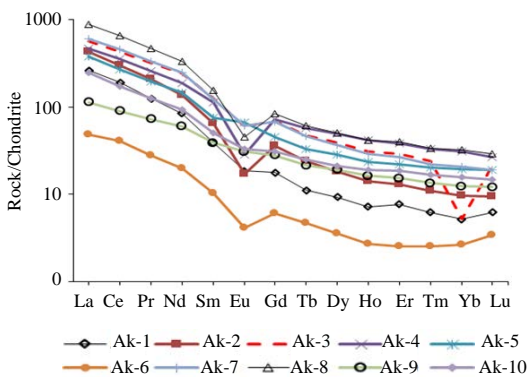

Fig. 21: Chondrite-normalized REE pattern of granite from Akure

11.41-38.87) and a distinct negative Eu anomaly (Eu/Eu* = 3.09-3.62). Table 6 indicates an enriched LREE (233.51-850.55) and an impoverished HREE (14.74-67.19). The summation of the REE range from 8.54-917.74. The Chondrite normalized REEs pattern display a high degree of fractionation (La/Yb) N = 11.66-49.67) with LREE/HREE ratio (8.42-15.84) and a strong negative Eu anomaly (Fig. 21). Drummond and Defant[38] and Martin *et al.*[39] reported that the depletion of HREE is predominantly caused by low degrees of melting of garnet-rich sources. In another development, Gromet and Silver[40] and Rollinson[41] suggested that depleted HREE could be caused by the late stage fractionation of heavy mineral phases like zircon, allanite, sphene, apatite and monazite because of their extremely high partition coefficients for HREE.

Table 5: Rare earth element abundance (ppm) of rock from Akure

La	61.8	58.58	132.7	243.45	102.6	116.8	213.8	181.1	121.4	217.15
Ce	116.05	106.42	219.2	390.9	196.65	219.3	384.75	342.75	211.85	379.3
Pr	11.57	11.67	24.53	43.99	21.47	23.58	39.97	36.26	21.45	41.16
Nd	38.35	42.25	82.9	149.4	76.4	82.65	134.8	126.55	72.3	140.15
Sm	5.74	7.38	12.75	22.81	12.55	14.01	20.53	21.07	9.86	22.49
Eu	5.74	7.38	12.75	22.81	12.55	14.01	20.53	21.07	9.86	22.49
Gd	3.55	6.09	9.48	16.27	9.30	12.46	15.65	15.79	6.69	16.63
Tb	0.4	0.91	1.10	2.11	1.26	1.78	1.93	2.07	0.84	2.22
Dy	2.29	5.17	5.78	11.18	7.1	10.91	10.51	10.74	4.48	12.39
Ho	0.40	1.03	0.91	2.04	1.37	2.16	1.93	2.03	0.86	2.41
Er	1.22	2.98	2.05	5.80	4.08	6.59	5.67	5.49	2.62	6.7
Tm	0.15	0.41	0.26	0.79	0.58	0.96	0.76	0.70	0.34	0.95
Yb	0.84	2.54	1.92	5.40	4.0	6.77	4.93	4.22	2.11	6.25
Lu	0.15	0.36	0.30	0.79	0.63	1.06	0.76	0.62	0.25	0.92
Y/Nb	1.39	2.43	4.84	5.60	6.52	4.00	7.03	3.14	3.57	4.49

Table 6: Chondrite normalized values for REE of Akure Pan African rocks

Samples	Ak1	Ak2	Ak3	Ak4	Ak5	Ak6	Ak7	Ak8	Ak9	Ak10
La	168.39	159.62	361.58	663.35	279.56	318.26	582.56	493.46	330.79	591.70
Ce	121.26	111.20	229.05	408.46	205.49	229.15	402.04	358.15	221.37	396.34
Pr	84.45	85.18	179.05	321.09	156.72	172.12	291.75	264.74	156.57	300.51
Nd	53.94	59.42	116.60	210.13	107.45	116.24	189.59	177.99	101.69	197.12
Sm	24.85	31.95	55.19	98.74	62.99	60.65	88.87	91.21	42.68	97.36
Eu	65.98	84.83	146.55	262.18	144.25	161.03	235.98	242.18	113.33	258.51
Gd	11.60	19.90	30.98	50.17	30.39	40.72	51.14	50.60	25.13	54.35
Tb	6.90	15.69	18.97	36.38	21.72	30.70	33.28	35.70	14.48	38.28
Dy	6.01	13.57	15.17	29.34	18.64	28.64	27.59	28.19	11.76	32.52
Ho	4.66	12.12	10.71	24.0	16.12	25.41	22.71	23.88	10.12	28.35
Er	4.90	11.97	8.23	23.29	16.39	26.47	22.77	22.05	10.52	26.91
Tm	4.17	11.5	7.22	21.94	16.11	26.67	21.11	19.44	9.44	26.39
Yb	3.39	10.24	7.74	21.77	16.13	27.30	19.88	17.02	8.51	25.20
Lu	3.95	9.47	7.89	20.79	16.58	27.89	20.00	16.32	6.58	24.21
LREE	233.51	226.3	472.08	850.55	410.67	456.34	793.85	707.74	436.86	800.25
HREE	14.74	26.87	34.55	67.19	40.87	63.22	62.67	62.73	29.05	70.96
REE	248.25	253.17	506.63	917.74	82.54	519.56	856.52	770.47	465.91	871.21
LREE/HREE	15.84	8.42	13.66	12.66	9.36	12.60	12.67	11.28	15.04	11.28
Eu/Eu*	3.62	3.27	3.40	3.52	3.09	3.18	3.37	3.39	3.34	3.42
(La/Yb)N	49.67	15.59	46.72	30.47	17.33	11.66	29.30	28.99	38.87	22.29
(La/Lu)N	42.63	16.86	45.83	31.91	16.86	11.41	29.13	30.24	50.27	24.44

The depletion of Ba (0.48-8.76) and the presence of negative Eu are suggestive of fractionation of both plagioclase and K-feldspar. The distinct negative Eu anomaly in the REE pattern (Fig. 21) is an indication of an extensive fractionation of plagioclase and this is corroborated by a strong negative correlation Al_2O_3 and CaO with SiO_2 in the variation diagram of Fig. 19. It is noted that all samples are generally enriched in light rare earth elements (LREE) and depleted relative to the heavy rare earth elements HREE (Fig. 21).

Tectonic discrimination and provenance: Roche et al.[42] proposed a tectonic classification scheme for volcanic and plutonic rocks based upon their cationic proportions of major elements. The diagram is an X-Y bivariate graph using the plotting parameters R1 and R2 where: R1 = 4Si -11 (Na+K)-2 (Fe+Ti) and R2 = Al+2Mg+6Ca) (Fig. 22). Batchelor and Bowden[43] showed that the diagram can discriminate five granitic groups related to the tectonomagmatic divisions as proposed by Pitcher[44, 45]. The granite samples plotted in the post collision uplift field and late orogenic
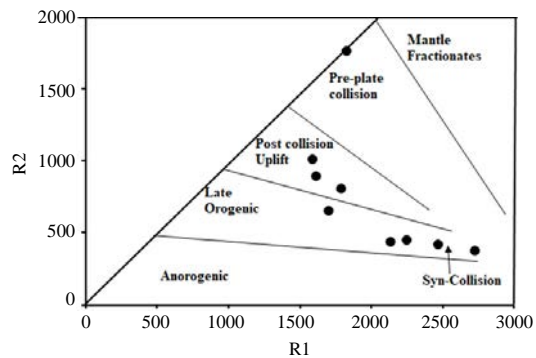

Fig. 22: R1 = (4Si-11(Na+K)-2(Fe+Ti)) vs. R2 = (Al+ 2Mg+6Ca) tectonic discrimination diagram for the granite rocks from the study area[46]; R1 = 4Si-11(Na+K)-2(Fe+Ti): R2 = 6Ca+2Mg+Al

fields, respectively (Fig. 22). The results agree with the age of the granite, magmatism and tectonic scenario of Pan African granite (Older granite) which took place in
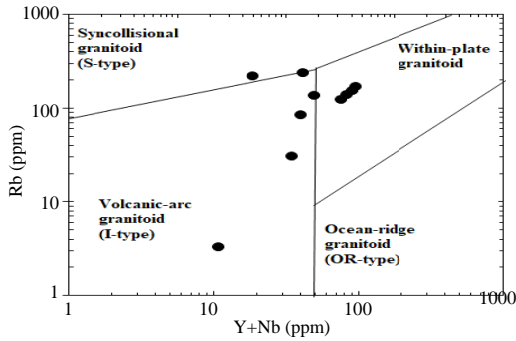
Fig. 23: Rb-(Y+Nb) discrimination diagram for the rocks from Akure[47] Syn-collisional granitoid; Within-plate granitoid; Ocean ridge granitoid; Volcanic arc granitoid
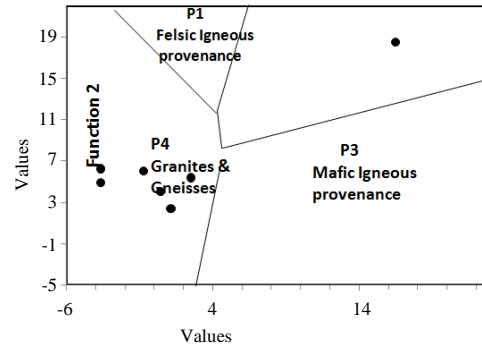

Fig. 25: Provenance signatures of Akure rocks indicating granite and gneisses sources[48]
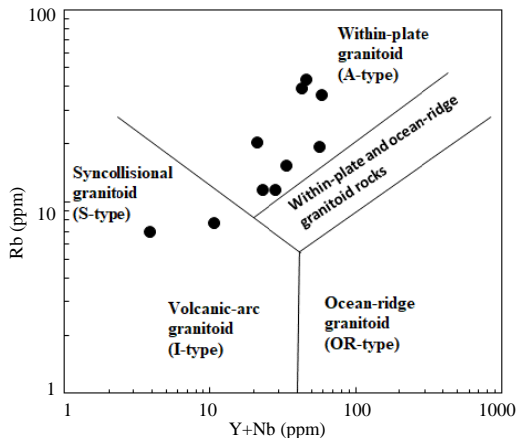

Fig. 24: Nb-Y discrimination diagram for the rocks[47]. Syn-collisional granitoid; Within-plate granitoid; Ocean ridge granitoid; Volcanic arc granitoid
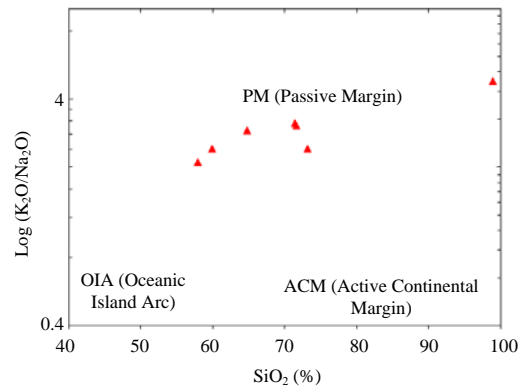

Fig. 26: Discrimination diagram of Roser and Korsch[49] showing the fields of oceanic island arc; active continental margin and passive margin

600±150 Ma. The granite samples plotted in the within-plate granitoid, (WPG) volcanic-arc granite (VAG) (I-Type) and syn-collisional granite, (Syn-COLG) fields of Rb-(Y+Nb) discrimination diagram of Peace *et al.*[47] (Fig. 23). The WPG, VAG and Syn-COLG fields or environments are supported by the tectonic discrimination plots of Nb versus Y of Peace *et al.*[47] (Fig. 24) as well as R1 versus R2 plots of Bowden *et al.*[46] (Fig. 22). The provenance of the rocks is affirmed by the discriminant diagram of Roser and Korsch[48] where the discriminant functions were used to define 4 main provenances (Fig. 25) namely; mafic igneous provenance; intermediate igneous provenance; felsic igneous provenance and granite and granites. Figure 25 shows clearly that the Pan African rocks so studied are of granites and granite gneisses provenance found in the

passive and active continental margins of the Earth in the diagram of K_2O/Na_2O against SiO_2 plots (Fig. 26). An active continental margin setting conforms to the calc-alkaline character of the samples with lower crust possible origin.

An attempt has been made in this study to show the different crystallizing options in the granite from Akure areas. A plot of TiO_2 versus Zr indicates the general trends of the granitic rocks as controlled by some sets of crystallizing minerals of zircon+sphene, zircon+ hornblende, zircon+magnetite, zircon+biotite+ hornblende and zircon+hornblende+sphene. Figure 27 is a plot of TiO_2 vs. Zr showing the granite trends where mineral vectors indicate the path evolved liquids for 15% for participating minerals: Pl = plagioclase; Kf = K-feldspar; Qz = quartz; Mt = magnetite; Sp = sphene; Hbl = hornblende; Bi = biotite; Zi = zircon. The samples have two crystallization trends.

In Fig. 27, trend 1 appears to be controlled by felsic minerals plagioclase, pl, potassium feldspar, kf and
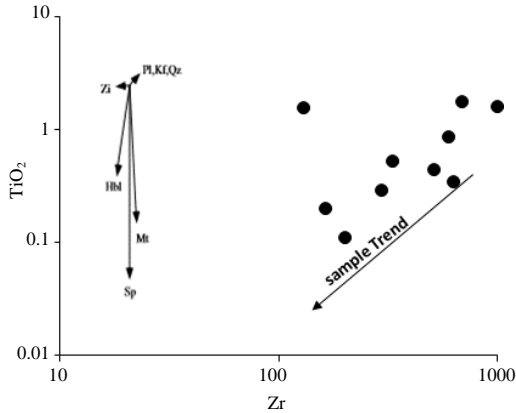
Fig. 27: A plot of TiO$_2$ vs. Zr showing the granite trends where mineral vectors indicate the path evolved liquids for 15% for participating minerals
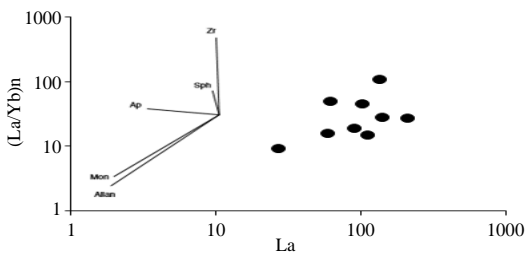

Fig. 28: (La/Yb)^n-La plot of the granitic rocks from Akure area

quartz, qz where as trend 2 is controlled by a combination of zircon Zr)+hornblende, (HN)+sphene, (Sp)+magnetite, (Mt).

Mineral vectors indicate paths evolved liquids for 15% of precipitating minerals: Pl = plagioclase; Kf = K-feldspar; Qz = quartz; Mt = magnetite. The essence of sphene, zircon, allanite, apatite and monazite is shown in the plot of (La/Yb)N versus La diagram (Fig. 28). The vector diagram shown in Fig. 28 represents a net change in composition of the liquid after 15% Rayleigh fractionation by removing sphene, zircon, allanite, apatite or monazite. The granitic samples show a scattered trend which makes it hard to predict their mineral crystallization options.

CONCLUSION

The results of the geochemical analysis of the granitic rocks show varying concentrations of the major oxides. Silica, SiO$_2$ (50.18-71.65) and alumina, A$_2$O$_3$ (0.26-17.29) are abundant in the rocks.as well as Fe$_2$O$_3$ (0.52-10.77) and potash, K$_2$O (0.07-5.98).The magma and the corresponding rocks are silica over-saturated and quartz-rich. The high value of the alumina, (Al$_2$O$_3$) 0.26-17.29 resembles those of the calc-alkaline rock series. The Alumina Saturation Index (ASI) characterized the rocks under study as peraluminous, S-Type, slightly metaluminuos, I-Type and A-Type granites. The F-S methods for finding the compositional equivalent of rock types from the study areas showed ultrafelsic granite, granodiorite, tonalite, all of the granite family. A plot of total alkalies-silica of alkaline and sub-alkaline rock suites indicated the rock types as granite, syenite, quartz-diorite, gabbro, monzogranite and monzodiorite. Different fields, so, plotted for the different rock types indicate different sources of origin. The sub-alkaline rocks showed evidence of crystal fractionation from a magmatic melt as supported by the decreasing trend of CaO, MgO, TiO$_2$ and Fe$_2$O$_3$ with increasing SiO$_2$, all indicating a characteristic of a fractionating granitic system. The depletion of Ba (0.48-8.76), the presence of distinct negative Euin the REE pattern, coupled with a strong negative correlation of Al$_2$O$_3$ and CaO with SiO$_2$ in the variation diagrams are suggestive of an extensive fractionation of plagioclase. The geochemical plots established the involvement of magmatic and tectonic activities with subsequent post collision uplift and late orogeny in conformity with tectonic scenario of Pan African granite (Older granite) which took place in 600±150 Ma. Also, the within-plate (WPG), volcanic-arc and syn-collisional tectonic regimes observed in the discrimination diagram of Pearce *et al.*[47] are characteristics typical of Pan African granitic rocks. These geodynamic activities resulted in the emplacement of rock suites namely: granite, syenite, quartz-diorite, gabbro, monzogranite and monzodiorite.

REFERENCES

01. Ajibaje, A.C., 1982. Origin and emplacement of older granites of Nigeria: Some evidence from Zungeru region. J. Min. Geol., 19: 221-230.
02. Balaram, V., S.L. Ramesh and K.V. Anjaiah, 1996. New trace element and REE data in thirteen GSF reference samples by ICP MS. Geostand. Newsl., 20: 71-78.
03. Norman, M.D., 1998. Melting and metasomatism in the continental lithosphere: Laser ablation ICPMS analysis of minerals in spinel lherzolites from Eastern Australia. Contrib. Mineral. Petrol., 130: 240-255.

04. Norman, M.D., N.J. Pearson, A. Sharma and W.L. Griffin, 1996. Quantitative analysis of trace elements in geological materials by laser ablation ICPMS: Instrumental operating conditions and calibration values of NIST glasses. Geostand. Newsl., 20: 247-261.

05. Obasi, R.A. and A.O. Talabi, 2019. Geochemistry and Feldspathic studies of pan-African granites around Ado-Ekiti, Ekiti State, Nigeria. Int. J. Sci. Eng. Res., 10: 1558-1581.

06. Irvine, T.N. and W.R.A. Baragar, 1971. A guide to the che-mical classification of the common volcanic rocks. Can. J. Earth Sci., 8: 523-548.

07. Pearce, J.A. and J.R. Cann, 1973. Tectonic setting of basic volcanic rocks determined using trace element analyses. Earth Planet. Sci. Lett., 19: 290-300.

08. Jakes, P. and A.J.R. White, 1971. Composition of island arcs and continental growth. Earth Planet. Sci. Lett., 12: 224-230.

09. Jakes, P. and A.R. White, 1972. Major and trace element abundances in volcanic rocks of orogenic areas. Geol. Soc. Am. Bull., 83: 29-40.

10. Nockolds, S.R., 1954. Average chemical compositions of some igneous rocks. Bull. Geol. Soc. Am., 65: 1007-1032.

11. Le Bas, M.J., R.W. Le Maitre and A.R. Woolley, 1992. The construction of the total alkali-silica chemical classification of volcanic rocks. Mineral. Petrol., 46: 1-22.

12. Williams, H., F.J. Turner and C.M. Gilbert, 1982. Petrography: An Introduction to the Study of Rocks in Thin Sections. W.H Freeman, New York, USA., Pages: 626.

13. Maitre, R.W. L., 1989. A Classification of Igneous Rocks and Glossary of Terms. Oxford Blackwell Scientific Publishers, New York, USA., Pages: 193.

14. Miyashiro, A., 1974. Volcanic rock series in island arcs and active continental margins. Am. J. Sci., 274: 321-355.

15. Shahabpour, J., 2007. Island-arc affinity of the central Iranian volcanic belt. J. Asian Earth Sci., 30: 652-665.

16. Loiselle, M. and D. Wones, 1979. Characteristics and origin of anorogenic granites. Geol. Soc. Am. Abstr. Programs, Vol. 11,

17. Frost, C.D. and R.B. Frost, 1997. Reduced rapakivi-type granites: The tholeiite connection. Geology, 25: 647-650.

18. Frost, B.R. and C.D. Frost, 2008. A geochemical classification for feldspathic igneous rocks. J. Petrol., 49: 1955-1969.

19. Roberts, M.P. and J.D. Clemens, 1993. Origin of high-potassium, calc-alkaline, I-type granitoids. Geology, 21: 825-828.

20. Ukaegbu, V.U., 2003. The petrology and geochemistry of parts of Obudu Plateau, Bamenda massif, Nigeria. Ph.D. Thesis, University of Port Harcourt, Port Harcourt, Nigeria.

21. Rickwood, P.C., 1989. Boundary lines within petrologic diagrams which use oxides of major and minor elements. Lithos, 22: 247-263.

22. Peacock, M.A., 1931. Classification of igneous rock series. J. Geol., 39: 54-67.

23. Frost, B.R., C.G. Barnes, W.J. Collins, R.J. Arculus and D.J. Ellis *et al.*, 2001. A geochemical classification for granitic rocks. J. Petrol., 42: 2033-2048.

24. Maniar, P.D. and P.M. Piccoli, 1989. Tectonic discrimination of granitoids. Geol. Soc. Mer. Bull., 101: 635-643.

25. Eby, G.N., 1990. The A-type granitoids: A review of their occurrence and chemical characteristics and speculations on their petrogenesis. Lithos, 26: 115-134.

26. Frost, C.D. and B.R. Frost, 2011. On ferroan (A-type) granitoids: Their compositional variability and modes of origin. J. Petrol., 52: 39-53.

27. Dall'Agnol, R. and D.C. de Oliveira, 2007. Oxidized, magnetite-series, rapakivi-type granites of Carajas, Brazil: Implications for classification and petrogenesis of a-type granites. Lithos, 93: 215-233.

28. Chappell, B.W. and A.J.R. White, 1974. Two contrasting granite types. Paciffic Geol., 8: 173-174.

29. Whalen, J.B., K.L. Currie and B.W. Chappell, 1987. A-type granites: Geochemical characteristics, discrimination and petrogenesis. Contrib. Mineral. Petrol., 95: 407-419.

30. Mohamed, F.H. and M.A. Hassanen, 1997. Geochemistry and petrogenesis of Sikait leucogranite, Egypt: An example of S-type granite in a metapelitic sequence. Geol. Rundschau, 86: 81-92.

31. White, W.M., 2004. Geochemistry. John-Hopkins University Press, New York, USA.,.

32. Eby, G.N., 1992. Chemical subdivision of the A-type granitoids: Petrogenetic and tectonic implications. Geology, 20: 641-644.

33. Tarney, J. and B.F. Windley, 1977. Chemistry, thermal gradients and evolution of the lower continental crust. J. Geol. Soc., 134: 153-172.

34. Taylor, S.R. and S.H. McLennan, 1995. The geochemical evolution of the continental crust. Rev. Geophys., 33: 241-265.

35. Shaw, A., H. Downes and M.F. Thirlwall, 1993. The quartz-diorites of Limousin: Elemental and isotopic evidence for Devono-Carboniferous subduction in the Hercynian belt of the French Massif Central. Chem. Geol., 107: 1-18.

36. Parada, M.A., J.O. Nystrom and B. Levi, 1999. Multiple sources for the Coastal Batholith of central Chile (31-34 S): Geochemical and Sr-Nd isotopic evidence and tectonic implications. Lithos, 46: 505-521.

37. Taylor, S.R. and S.M. McLennan, 1981. The composition and evolution of the continental crust: Rare earth element evidence from sedimentary rock. Phil. Trans. R. Soc., 301: 381-399.

38. Drummond, M.S. and M.J. Defant, 1990. A model for trondhjemite tonalite dacite genesis and crustal growth via slab melting: Archean to modern comparisons. J. Geophys. Res. Solid Earth, 95: 21503-21521.

39. Martin, H., R.H. Smithies, R. Rapp, J.F. Moyen and D. Champion, 2005. An overview of adakite, Tonalite-Trondhjemite-Granodiorite (TTG) and sanukitoid: Relationships and some implications for crustal evolution. Lithos, 79: 1-24.

40. Gromet, L.P. and L.T. Silver, 1983. Rare earth element distributions among minerals in a granodiorite and their petrogenetic implications. Geochim. Cosmochim. Acta, 47: 925-939.

41. Rollinson, H.R., 1993. Using Geochemical Data. Longman Scientific and Technical Insitute, UK., ISBN-10: 0582067014, pp: 352.

42. Roche, D.H.D.L., J.T. Leterrier, P. Grandclaude and M. Marchal, 1980. A classification of volcanic and plutonic rocks using R1R2-diagram and major-element analyses-its relationships with current nomenclature. Chem. Geol., 29: 183-210.

43. Batchelor, R.A. and P. Bowden, 1985. Petrogenetic interpretation of granitoid rock series using multicationic parameters. Ehem. Ged., 48: 43-55.

44. Pitcher, W.S., 1979. The nature, ascent and emplacement of granitic magmas. J. Geol. Soc., 136: 627-662.

45. Pitcher, W.S., 1983. Granite Type and Tectonic Environment. In: Mountain Building Processes, Hsu, K. (Ed.). Academic Press, London, England, UK., pp: 19-40.

46. Bowden, P., R.A. Batchelor, B.W. Chappell, J. Didier and J. Lameyre, 1984. Petrological, geochemical and source criteria for the classification of granitic rocks: A discussion. Phys. Earth Planet. Inter., 35: 1-11.

47. Pearce, J.A., N.B.W. Harris and A.G. Tindle, 1984. Trace element discrimination diagrams for the tectonic interpretation of granitic rocks. J. Petrol., 25: 956-983.

48. Roser, B.P. and R.J. Korsch, 1988. Provenance signatures of sandstone-mudstone suites determined using discriminant function analysis of major-element data. Chem. Geol., 67: 119-139.

49. Roser, B.P. and R.J. Korsch, 1986. Determination of tectonic setting of sandstone-mudstone suites using SiO_2 content and K2O/Na2O ratio. J. Geol., 94: 635-650.